Science of Sintering, **55** (2023) 509-519

https://doi.org/10.2298/SOS220624020N

UDK: 535.375; 678.7; 77.026.34

Changes in the Physicochemical Properties of Geopolymer Gels as a Function of NaOH Concentration

Miloš Nenadović[1*)], Marija Ivanović[2], Danilo Kisić[1], Nenad Bundaleski[1,3], Vera Pavlović[4], Sanja Knežević[2], Ljiljana Kljajević[2]

[1]Department of Atomics Physics, Vinča Institute of Nuclear Sciences, National Institute of the Republic of Serbia, Mike Petrovića Alasa 12-14, Vinča, 11000 Belgrade, Serbia

[2]Department of Materials, Vinča Institute of Nuclear Sciences, National Institute of the Republic of Serbia, University of Belgrade, Mike Petrovića Alasa 12-14, Vinča, 11000 Belgrade, Serbia

[3]CEFITEC, Departamento de Física, Faculdade de Ciências e Tecnologia, Universidade Nova de Lisboa, Portugal

[4]University of Belgrade, Faculty of Mechanical Engineering, Kraljice Marije 16, 11120 Belgrade, Serbia

Abstract:

In the present paper, polymerization of alkali activated metakaolin (MK) and its structural changing, using 2M NaOH, 8M NaOH, and 16M NaOH solutions were followed by means of X-ray photoelectron spectroscopy (XPS), Diffuse reflectance infrared Fourier transform spectroscopy (DRIFT), Raman spectroscopy and Scanning electron microscopy (SEM). XPS analysis revealed that changing of NaOH concentration did not affect the types of formed bonds in the material. At the same time, the amount of sodium and aluminum increased with the NaOH molarity. The latter steps could be especially interesting because it may indicate the possibility of 'dosing' the amount of Al incorporated by changing the NaOH concentration in the solution. DRIFT analysis revealed that the absorption band for Al^{IV} located at 800 cm^{-1} is shifted towards the smaller values. Changing the concentration of NaOH, the chemical content did not change, but the structural changes are observed. Raman spectroscopy detected that the most dominant peaks at ~400 cm^{-1} and 519 cm^{-1} originate from Si-O-Al and Si-O-Si bending modes. With increasing the NaOH concentration, peaks at 1019-1060 cm^{-1} become more prominent as a result of polymerization. Both analyzes (DRIFT and Raman) confirmed the presence of quartz. SEM analysis showed that different structures are created by changing the concentration of NaOH.

Keywords*: Metakaolin; Geopolymer; NaOH; X-ray photoelectron spectroscopy (XPS), Raman spectroscopy.*

1. Introduction

In recent years, there has been great interest in alkaline activated materials (AAM). Alkaline-activated materials are increasingly used and researcher's interests are greater for this class of material in the previous period [1-7]. In addition to the natural raw materials u

*) **Corresponding author:** milosn@vin.bg.ac.rs

Increasingly sophisticated methods are confirming the polymerization mechanisms that are still under discussionare still under discussion are being confirmed by increasingly sophisticated methods. The alkali activation process is a chemical reaction between aluminosilicate - oxides and alkali metal silicate solutions under a very alkaline condition, where a three-dimensional geopolymer structure is obtained as the product [8-10].

Alkaline activated materials, a new class of alumino-silicate materials, are attractive because of their excellent mechanical properties, durability and thermal stability. In addition, they are of great interest due to the reduced energy requirement for their manufacture and the high sustainability. AAM are a new class of materials obtained by activation of inorganic precursors mainly constituted of silica, alumina, and low calcium oxide content. Activation occurs thanks to the use of strong alkaline solutions such as NaOH, KOH, and those of sodium silicate. Unlike other industrial processes (e.g., sol-gel, clinkerization, sintering processes), alkali activation process does not require expensive chemical reagents, use of carbonate-based raw materials or high temperature thermal treatments. The consolidation process of the activated precursors occurs at room temperature or by curing at a temperature lower than 100 °C. The most recent investigations highlight the alkali activation process as one of the possible routes towards the production of novel ceramic materials consolidated at low temperature [2]. Furthermore, it is possible to produce controlled porosity components by introducing foaming agents to the mixture at the fluid state, before hardening, and by controlling the thermal curing cycle. The possibility of using various kinds of aluminosilicate materials as a raw material to produce new ceramic materials for specific applications involves several advantages such as: (i) saving not renewable resources and, consequently, their safeguard; (ii) reducing CO_2 emission and, consequently, a good action on climate change; (iii) producing materials with excellent mechanical, adsorption, exchange and thermal properties. The resulting three-dimensional structure consists of Si – O – Al groups arranged in several phases: amorphous, semi-crystalline and one or more crystalline phases [3]. Our previous research [2, 13] confirmed that the chemical and mineralogical composition does not change with the aging of samples, but the structure of the material, as well as its properties, is modified. These studies followed the polymerization process by day (after 7, 14, 21 and 28 days) and it was concluded that the mineralogical composition did not change and that with the aging of the samples, a more compact and solid material was obtained [14]. Additional studies using FTIR and MALDI-TOF methods confirm that material structure is changing [15]. Also, a description of the aging of geopolymer made from fly ash is presented in the paper of A. Savić et. al. [33] Apart from the structure modification, changing the NaOH concentration also affects the radiological properties [3]. Raman spectroscopy has been used in several studies on silicate solutions [16–18] to investigate the effects of different parameters, such as the contributions of monomers and oligomers [18, 19].

The aim of this paper is to examine the structural changes in alkali activated metakaolin that occur after the polymerization process, initiated by different concentrations of NaOH. For that purpose, the samples were subjected to different NaOH solutions, enabling to follow structural, chemical, and physical changes of geopolymers using various experimental techniques. The obtained result open a perspective to optimize the structural properties of alkali activated metakaolin by controlling the amount of NaOH in the solution.

2. Materials and Experimental Procedures

2.1. Materials and methods

Metakaolin was obtained from kaolin by thermal treatment at 750°C. Previous FTIR studies have shown, that Al^{IV} absorption band was at 800 cm^{-1} [15]. Alkaline activation in 2M NaOH, 8M NaOH, and 16M NaOH solution leads to the formation of geopolymer materials

denoted as GP2M, GP8M, and GP16M, respectively. All samples were synthesized under the same conditions, and after complete polymerization of the alkali-activated material (28 days), DRIFT, Raman spectroscopy, XPS, and SEM analysis were conducted in order to reveal the differences between the as-synthesized samples.

2.2. Characterization

2.2.1. XPS (X-ray photoelectron spectroscopy) analysis

Surface characterization was conducted using a SPECS instrument for XPS analysis. The powder samples were subjected to thermal treatment for 3 h at 90°C in air, and amount of adsorbed water was sufficiently reduced to allow the measurements. Shortly after, samples were removed from the furnace, attached on an adhesive tape, and introduced into the vacuum load lock and analyzing chamber.

Photoelectron emission was obtained from aluminum anode excited by monochromatic Al Kα line with photon energy of 1486.67 eV. Survey spectra were recorded prior to detailed spectra. The main photoelectron lines of detailed spectra were acquired in the fixed analyzer transmission mode with pass energy of 20 eV (FAT 20), an energy step of 0.1 eV and a dwell time of 2 s. Electron flood gun was used for charging compensation of the samples showing insulating properties. Binding energy axis was calibrated from the C 1s line position, assuming that it corresponds to adventitious carbon situated at 284.8 eV. The atomic sensitivity factors which are provided by the manufacturer were used for the composition analysis according to the characteristic photoelectron line intensities. The fitting of photoelectron lines was done using pseudo-Voigt GL (30) (30% Lorentzian, 70% Gaussian) profiles. FWHM of contributions from the same photoelectron line were assumed to be constant during the fitting. Ratio between the $2p_{3/2}$ and $2p_{1/2}$ photoelectron lines corresponding to the same bond were fixed to the theoretical 2:1, while the spin-orbit splitting in Al 2p and Si 2p lines was fixed to 0.44 eV and 0.63 eV, respectively.

2.2.2. DRIFT analysis

In this paper, the structural analysis of the samples was monitored using DRIFT analysis. All samples were turned into a fine powder and dispersed homogeneously into anhydrous potassium bromide (KBr) pellets (1.5 mg/150 mg KBr). A more detailed description of the methods used is presented in the paper Nenadović et al. [20]

2.2.3. Raman spectroscopy

Raman spectroscopy of geopolymer samples were acquired on a LabRAM HR Evolution equipment. The working range was from 200 up to 1200 cm^{-1}, by using 532 nm laser line. Spectrometer is equipped with a grating acquiring 1800 lines/mm and with 100× microscope lens. Acquisition integration time was kept constant at 60s/4 cycles, while power applied on a sample was 25 mW.

2.2.4. Scanning electron microscopy

In order to analyze the microstructure and morphology of the surface of the samples, the SEM analysis method was used. The analysis was done using field emission scanning electron microscopy (FESEM, Tescan MIRA 3 KSMU) at 20 kV. Before the analysis, the samples were coated with Au/Pd alloy by sputtering.

3. Results and Discussion

3.1. XPS analysis

XPS analysis was performed on metakaolin samples treated with 2M NaOH (GP2M), 8M NaOH (GP8M), and 16M NaOH (GP16M). The composition of the four samples obtained using atomic sensitivity factors is summarized in Table I. The metakaolin used in these experiments is accompanied by a quartz phase. The third chemical phase in all samples are organic impurities, as evidenced by the presence of carbon. Since quantitative composition analysis of multiphase systems cannot be performed correctly using this approach, the data presented in Table I can be only considered as a relative measure and general trends of the composition changes with the molar content of NaOH.

Tab. I Composition of samples based on the intensity of dominant photoelectron lines.

Sample	C (%)	O (%)	Si (%)	Al (%)	Na (%)
GP2M	11.0	53.7	26.2	6.0	3.1
GP8M	4.3	55.1	24.7	11.6	4.3
GP16M	5.5	55.3	22.5	11.5	5.2

The composition of the samples GP8M and GP16M is identical in the frame of the experimental error, suggesting that doubling the NaOH content did not affect the synthesized material. However, we clearly see drop of Na, but also of Al, if NaOH content is further reduced. This result is particularly interesting, since one can apparently tune the amount of, not only Na but also Al incorporated into the geopolymer structure, by adjusting the alkaline solution. At the moment, the mechanism behind this effect is unclear. One possible explanation could be changing the pH of a solution affects the precipitation rate of aluminum.

In our previous work, we developed a consistent peak model for geopolymer samples [13]. Al $2p_{3/2}$ and Si $2p_{3/2}$ lines are expected at about 74.5 eV and 102.4 eV, respectively. Another silicon phase i.e. quartz, is also present, with Si $2p_{3/2}$ photoelectron line situated at about 103.5 eV. Particularly significant is O 1s line which consists of three contributions related to the –ONa group (O1 at ~ 529.6 eV), the sialate-siloxo group (O2 at ~ 531.2 eV) and the Si-OH group and quartz (O3 at ~ 532.8 eV). In this particular set of samples, we observe differential charging between the geopolymers and quartz, the latter resolves Si-OH contribution from geopolymers from the quartz contribution in O 1s. The original peak model is therefore modified in order to consider this fact: O 1s line was fitted to 4 contributions. The fourth peak corresponds to quartz, with the position defined relative to that of the Si $2p_{3/2}$ contribution of quartz: O4 – Si2 = 429.4 eV. The intensity of the peak O4 is calculated from that of Si2, using the previously determined composition of the quartz phase, $SiO_{1.8}$ [13]. Apart from this constraint for the O4 peak, all other oxygen contributions were fitted as free parameters. The results of the fitting are shown in Table II.

The positions of the Al $2p_{3/2}$ and Si $2p_{3/2}$ lines and of the contributions O1-3 practically coincide with the expected positions for the same type of geopolymers [13], thus justifying the applied fitting procedure. This is also a clear indication that amount of NaOH in the solution does not affect the chemical bonds formed in this phase. The only exception could be the position of the Si1 contribution, which shifted for about 0.4 eV towards higher binding energies in the GP2M sample, in which the amount of Al is significantly reduced (Table I). From the known intensities of the Si 2p and Al 2p lines attributed to geopolymer, we determined the Si:Al ratio in this phase using the corresponding atomic sensitivity factors. In this particular case the approach is correct, since we compare signals originating from the same chemical phase. Besides, difference between the signal attenuation of the two lines, e.g. due to the hydrocarbon overlayer, can be readily neglected due to the similar kinetic energies of the corresponding photoelectrons (~1407 eV and ~1380 eV of Al 2p and Si 2p lines,

respectively). In final, we estimate the Si:Al ratio to 1.56 in GP8M and GP16M, and to 4.05 in GP16M.

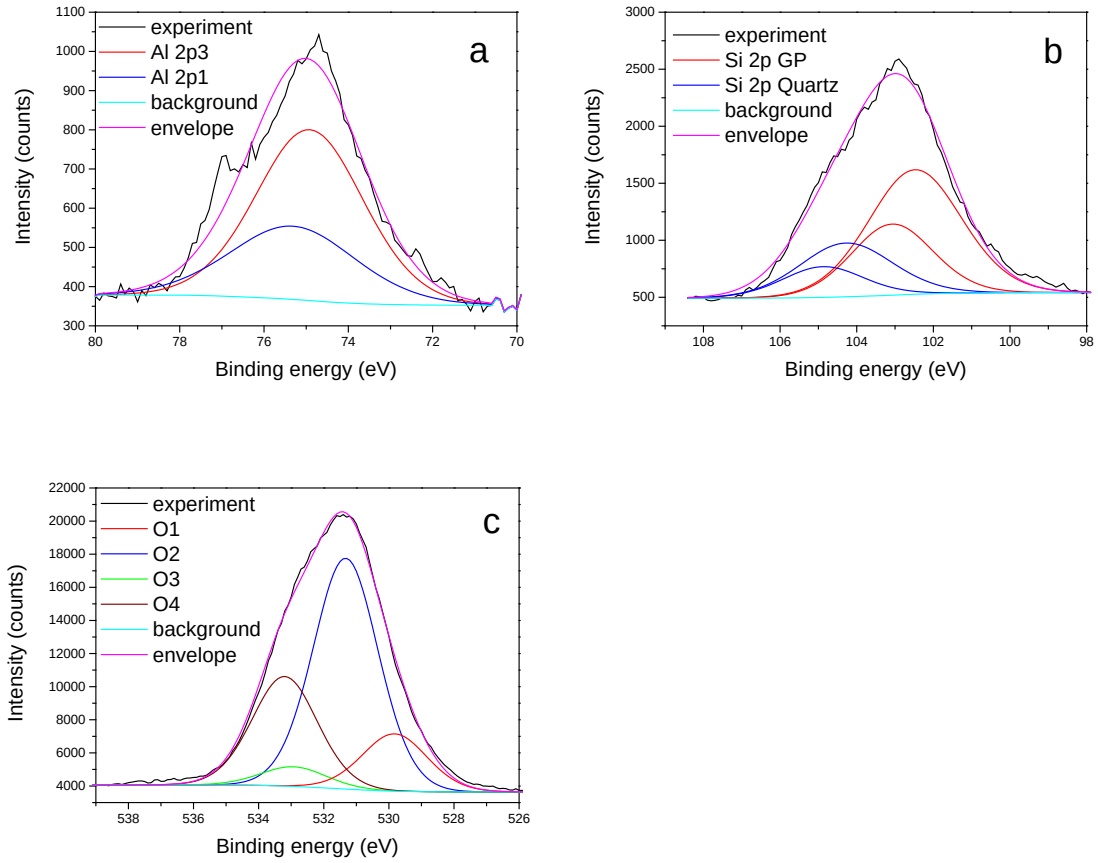

Fig. 1. High resolution XPS spectra of: a) Al 2p, b) Si 2p and c) O 1s photoelectron lines taken from GP8M sample, and the corresponding fittings.

Tab. II High resolution spectra fitting results of photo-electronic lines of geopolymer samples.

Sample	**O 1s (eV/%)**				**Si $2p_{3/2}$ (eV/%)**		**Al $2p_{3/2}$ (eV/%)**
	O1	**O2**	**O3**	**O4**	**Si1**	**Si2**	
GP2M	529,6/5,0	531,2/79,6	532,8/9,4	533,9/6,0	102,7/94,0	105,1/6,0	74,4
GP8M	529,8/13,7	531,3/55,3	532,9/4,7	533,8/26,3	102,4/62,2	104,2/37,8	75,0
GP16M	529,8/13,7	531,2/60,5	532,7/9,8	533,1/16,0	102,3/79,8	103,9/20,2	74,6

3.2. DRIFT analysis

The effect of chemical structure changing with increasing the NaOH concentration during the geopolymerization can be observed from Fig. 2. The broadening of absorption bands is more pronounced using higher concentration 8M and 16M of NaOH.

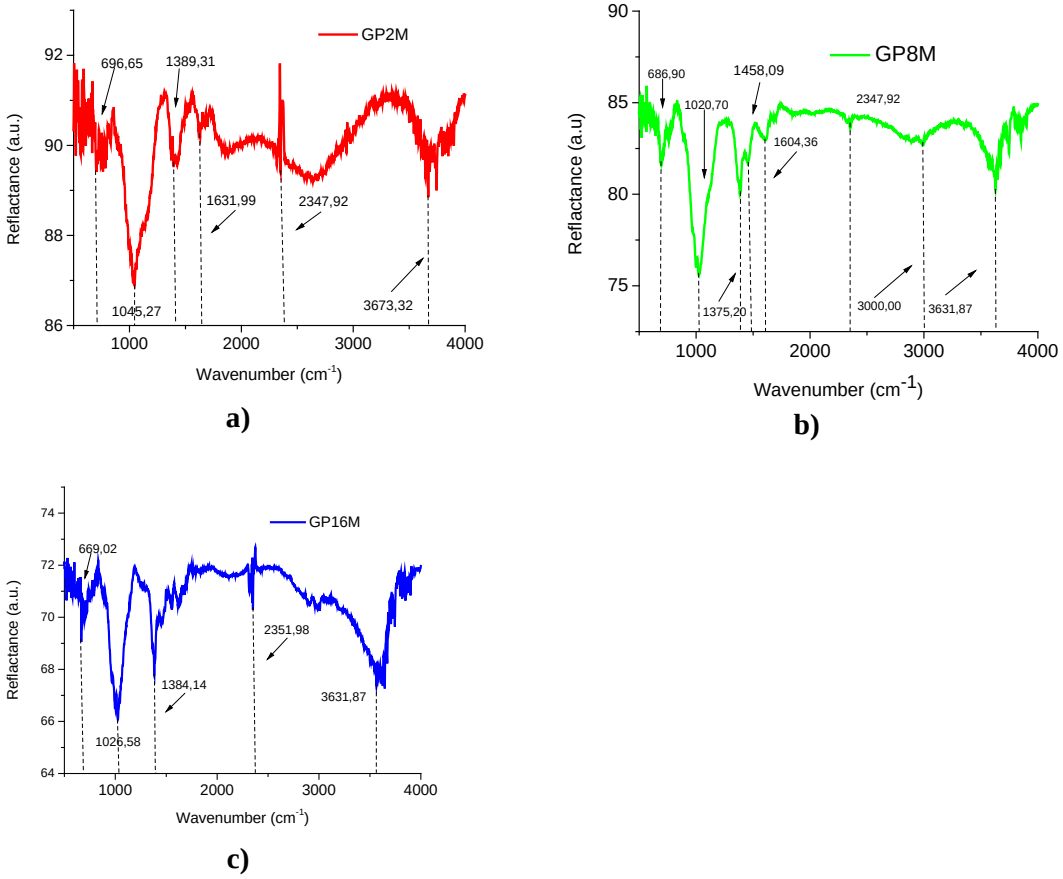

Fig. 2. DRIFT spectra of obtained geopolymers (GP) with different NaOH concentrations: a) GP2M, b) GP8M and c) GP16M.

The expected Al^{IV} absorption, has been detected at 793 cm^{-1}, after the geopolymerization process. The presence of quartz was confirmed by bands at 793 cm^{-1}, 692 cm^{-1},558 cm^{-1} and 445 cm^{-1}. These bands originate from two types of Si – O deformation vibrations - Si with basal O (793 cm^{-1}) for GP2M and Si with apical O (692 cm^{-1}, 558cm^{-1} and 445 cm^{-1}) for GP 8M and GP16M. In the region of Si-O valence vibration bands, pronounced peak was observed at 1015 cm^{-1}, which originates from the stretching of the Si bond with the apical and basal O in the plane. Weak band intensities of all samples were detected at 1635 cm^{-1} originating from OH valence and HOH deformation vibrations of adsorbed water.

The most interesting are bands at 793 cm^{-1} and 692 cm^{-1} in the GP spectrum. According to the literature data, in the region from 800 cm^{-1} up to 550 cm^{-1}one can find vibration bands that belong to Secondary Building Units (SBUs). SBUs consists of interconnected SiO^4 and AlO^4 tetrahedral structures, creating different merged rings [21, 22]. Observing the given spectra, it is noticed that all the bands are shifted to the right. The Al-O band at 793 cm^{-1} (GP2M) is slightly shifted as well as the band at 692 cm^{-1} (GP8M). There is a trend of new bands shifted to the right with increasing concentration of NaOH with formation of Si–O–Al (Si) bond band.

3.3. Raman spectroscopy analysis

Sample analysis using Raman spectroscopy shows that geopolymers examined have spectra that can be compared with the silicates, particularly the silicate glasses. As is known,

silicate glass creation consists out of a controlled modification of the 3D Si-O network by replacement of Si^{4+} covalent bonded atoms by noncovalent bonded atoms, hence decreasing the number of Si-O bridges and the connectivity of the network [14].

The results of Raman spectroscopy of geopolymer samples are reported in Fig. 3. In the sample GP2M the main Raman peaks are located at 357 cm^{-1} and 399 cm^{-1}. The first peak can originate from the Si-O and/or Al-O vibrations, the Na-O modes contribute to it as well [21, 23-25], while the second peak corresponds to the bending modes of Si-O-Al [24]. Although The shoulder at ~ 429 cm^{-1} can be induced by Si-O symmetric ring-breathing vibrations in a 5-fold or more-fold planar rings. However, some of the authors have assigned this peak to the asymmetric bending modes [23]. The peak at 585-600 cm^{-1} can be associated not only to the deformation of the bridging oxygen (BO) bonds in X-O-X (X: Si or Al) and to a rocking motion of BO in structural units that contain nonbridging oxygen (e.g. in structural units with NBO/X =1), [25], but also partly to the ring-breathing mode of three-membered rings, $D_2(\delta[R_3])$ [22, 27].

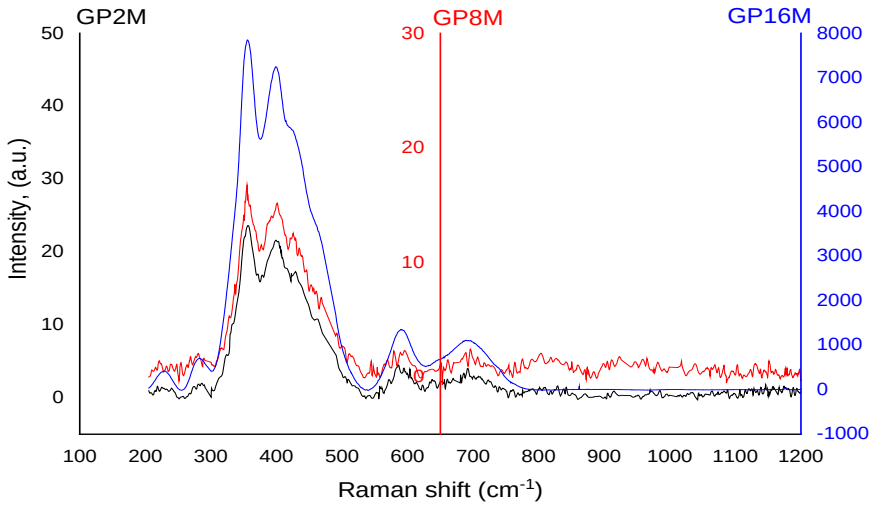

Fig. 3. Raman spectroscopy of geopolymer samples.

In the literature, it is often mentioned that the rage of 700-900 cm^{-1} corresponds to symmetric Si-O or Al-O stretching modes [24]. Furthermore, it is indicated that the peak at ~700 cm^{-1} can dominantly correspond to the contribution of 4-member rings. It should be noticed that the peak which covers the bands at 790 and 802 cm^{-1} can be primarily attributed to Si-O-Si bending symmetric modes in geopolymers [25, 26]. Some authors [26-28] pointed out that a peak at 780 cm^{-1} originates from the vibrations of Si-O-Si network and AlO_4 units with three bridging oxygens (BO) and one nonbridging (NBO). In addition, modes corresponding to Si-OH stretching vibration of $SiO(OH)_3^-$ can also contribute to this peak [29, 30]. The shoulder at 460-470 cm^{-1} that is detectable in the geopolymer samples, could be related to the position of the strongest α-quartz mode, which is usually assigned to the symmetric stretching Si-O-Si vibrations within the SiO_4 tetrahedron which was confirmed by DRIFT methods. As the molar concentration of NaOH increases, we see that there are no significant changes in the peaks in GP8M and GP16M, the peaks become clearer and more linear. In the GP16M sample, we notice that after 760 cm-1 there are no more peaks, which may be an indication that all MK reacted. In the paper Ivanović et al., a more detailed analysis of metakaolin is presented.

3.4. SEM analysis

SEM analysis was performed to identify the metakaolin reactants on the alkaline activator and to verify the internal microstructure. During the process of geopolymerization, different types of morphology were created. Fig. 4 shows the surfaces of the analyzed samples. Sodium hydroxide alkaline activator dissolved metakaolin particle, and that process leads to the formation of an inorganic polymer gel phase [31]. By using different concentrations of NaOH, different microstructures are formed.

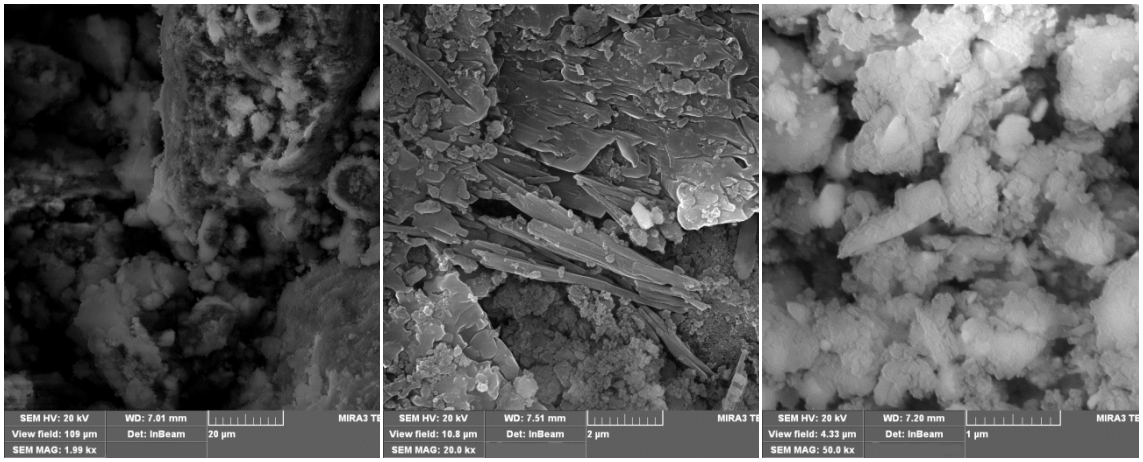

a) **b)** **c)**

Fig. 4. SEM microphotographs of geopolymer samples a) GP2M, b) GP8M, c) GP16M.

Fig. 4a shows the morphology of the GP2M sample. The analyzed sample shows a foam structure, on the basis of which it is assumed that the metakaolin hardening process is incomplete, which leads to incomplete geopolymerization. It is evident that the structure of GP2M is much weaker compared to other samples. The layered porous gel structure of sample GP8M is shown in Fig. 4b. There are also a large number of individual particles. The samples show a porous microstructure formed by unreacted micron size particles and geopolymer matrices formed during polycondensation. Based on the images, one can see that with the increase of NaOH, the newly formed sample contains part of the structure of the sample with a lower concentration of NaOH, that a new structure is formed and those two parts of the sample represent the newly formed structure. GP8M (Fig. 4b) shows that the microstructure consists of a dense plate formed by geopolymerization of metakaolin. However, the geopolymer dense sheets observed indicate that these are the strongest constituents. Finally, the sample that was polymerized with the highest concentration of NaOH - GP16M (Fig. 4c) shows more pronounced copolymer crystallites with a tendency to form dendritic structures. It is obvious that the concentration of the activator plays a significant role in the structure of the geopolymer and that with an increase in its concentration comes an increase in the degree of crystallinity, while GP2M and GP8M show a more amorphous and foamy structure.

4. Conclusion

The influence of NaOH concentration in both previous and these studies confirmed occurrence of crosslinking higher degree of aluminosilicate materials. X-ray photoelectron spectroscopy (XPS) analysis confirmed an increase in the Si:Al ratio from 1.56 to 4.05, which

further supports the fact that the degree of crosslinking has increased. It was also shown using the XPS method that there was no change in chemical bonds with increasing NaOH concentration. DRIFT analysis confirmed that there has also been a change in the structure of geopolymers through the broadening of absorption bands. It has been observed that with increasing NaOH concentration, the absorption bands shift to the right.

Raman spectroscopy revealed an interesting behavior of a geopolymer crosslinked with a higher concentration of NaOH. This is where vibrations of the Si-O-Si network and AlO_4 units with three bridging oxygens (BO) and one nonbridging (NBO) occur. As the concentration of alkali increases, the peaks of the Raman spectrum become more and more pronounced, and at wavelengths over 800 cm^{-1} there are no more peaks, which indicates that all metakaolin has reacted.

Scanning electron microscopy confirmed structural changes in all samples. Depending on the hydroxide concentration, various structural phenomena occur in geopolymers. At the lowest concentration, a foamy structure is observed, while with increasing concentration, a more compact and crystalline structure appears.

All applied characterization methods have shown that they are complementary in the case of characterization of this system and that there is indeed a change in the degree of crosslinking with increasing sodium hydroxide concentration.

Acknowledgments

This work was financially supported by the Ministry of Education, Science and Technological Development of Republic of Serbia on the research program grant No. 0402205 and grant No. 1702202, Vinča Institute of Nuclear Sciences, National Institute of the Republic of Serbia, University of Belgrade, Serbia.

5. References

1. J. Davidovits, S. Quentin, Geopolymers: Inorganic polymeric new materials, J. Therm. Anal. Calorim. 37 (1991) 1633-1656.

2. Lj. Kljajević, Z. Melichova, D. Kisić, M. Nenadović, B. Todorović, V. Pavlović, S. Nenadović, The influence of alumino-silicate matrix composition on surface hydrophobic properties, Science of Sintering, 51 (2) (2018) 163-173.
3. W.K.W Lee, J.S.J. van Deventer, Use of infrared spectroscopy to study geopolymerization of heterogeneous amorphous aluminosilicates, Langmuir, 19 (2003) 8726-8734.
4. C.A. Rees, J.L. Provis, G.C. Lukey, J.S.J. van Deventer, Attenuated total reflectance Fourier transform infrared analysis of fly ash geopolymer gel aging, Langmuir, 23 (2007) 8170-8179.
5. W.K.W. Lee, J.S.J. van Deventer, The effects of inorganic salt contamination on the strength and durability of geopolymers, Colloids Surfaces A – Physicochem. Eng. Aspects, 211 (2002) 115-126.
6. Y. Zhao, S. Kang, L. Qin, W. Wang, T. Zhang, S. Song; S. Komarneni, Self-assembled gels of Fe-chitosan/montmorillonitenanosheets: dye degradation by the synergistic effect of adsorption and photo-Fenton reaction, Chem. Eng. J.,379 (2020) 122322.
7. S. Kang, Y. Zhao, W. Wang, T. Zhang,T. Chen, H. Yi, F. Rao, S. Song, Removal of methylene blue from water with montmorillonitenanosheets/chitosan hydrogels as adsorbent, Appl. Surf. Sci.,448 (2018) 203-211.

8. W. Wang, Y. Zhao, H. Bai, T. Zhang, V. Ibarra-Galvan, S. Song, Methylene blue removal from water using the hydrogel beads of poly(vinyl alcohol)-sodium alginate-chitosan-montmorillonite, Carbohydr. Polym., 198 (2018) 518-528.
9. J. Peyne, J. Gautron, J. Doudeau, E. Joussein, S. Rossignol, Influence of calcium addition on calcined brick clay based geopolymers: a thermal and FTIR spectroscopy study, Constr. Build. Mater., 152 (2017) 794-803.
10. T. Zhang, Y. Zhao, S. Kang, Y. Li, Q. Zhang, Formation of active Fe(OH)3 in situ for enhancing arsenic removal from water by the oxidation of Fe(II)in air with the presence of $CaCO_3$, J. Clean Prod., 227 (2019) 1-9.
11. M. Ivanović, Lj. Kljajević, M. Nenadović, N. Bundaleski, I. Vukanac, B. Todorović, S. Nenadović, Physicochemical and radiological characterization of kaolin and its polymerization products, Mater. de Construction, 68 (2018) 330.
12. Lj. Kljajević, S. Nenadović, M. Nenadović, N. Bundaleski, B. Todorović, V. Pavlović, Z. Rakočević, Structural and chemical properties of thermally treated geopolymer samples, Ceramics International, 43 (9) (2017) 6700-6708.
13. S. Nenadović, G. Musci, Lj. Kljajević, M. Mirković, M. Nenadović, F. Kristaly, I. Vukanac, Physicochemical, minerological and radiological properties of red mud samples as secondary raw materials, Nuclear Technology and Radioactivity Protection, 32 (3) (2017) 261-266.
14. M.Ivanović, Lj. Kljajević, J. Gulicovski, M. Petković, I. Jankovic-Castvan, D. Bučevac, S. Nenadović, The effect of the concentration of alkaline activator and aging time on the structure of metakaolin based geopolymer, Science of sintering, 52 (2020) 219-229.
15. P. Duxson, J.L. Provis, G.C. Luckey, The role of inorganic polymer technology in the development of “green concrete”, Cem. Concr. Res., 37 (12) (2007) 1590-1597.
16. S.A. Bernal, R.M. de Gutierez, A.L pedraza, J.L. Provis, E.D Rodriguez, S. Delvasto, Effect of binder content on the performance of alkaliactivated slag concretes, Cem. Concr. Res., 41 (1) (2011) 1-8.
17. F. Pacheco-Torgal, D. Moura, Y. Ding, S. Jalal, Composition, strength and workability of alkali activated metakaolin based mortars, Constr. Build. Mater. 25 (9) (2011) 3732-3745.
18. M.R. El-Naggar, M.I. El-Dessouky, Re-use of waste glass in improving properties of metakaolin-based geopolymers: Mechanical and microstructure examinations, Construction. Build. Mater., 132 (2017) 543-555.
19. S. Nenadović, Lj. Kljajević, M. Ivanović, M. Mirković, N. Radmilović, L. Rakočević, and M. Nenadović, Structural and Chemical Properties of Geopolymer Gels Incorporated with Neodymium and Samarium, Gels, 7 (4) (2021) 195.
20. A.Fernández-Jiménez, A.Palomo, Mid-infrared spectroscopic studies of alkaline activated fly ash structure, Micropor Mesopor Mater, 86 (2005) 207-214.
21. M. Alkan, C. Hopa, Z. Yilmaz, H. Guler, The effect of alkali concentration and solid/liquid ratio on the hydrothermal synthesis of zeolite NaA from natural kaolinite, Microporous Mesoporous Materials, 86 (2005) 176-184.
22. T. Kosor, B. Nakic-Alfirević, S. Svilović, Geopolymer depolymerization index, Vibrational Spectroscopy, 86 (2016) 143-148.
23. L. Vidal, A. Gharzouni, E. Joussein, M. Colas, J. Cornette, J. Absi and S. Rossignol, Determination of the polymerization degree of various alkaline solutions: Raman investigation, J. Sol-Gel Sci. Technol. 83 (2017) 1-11.
24. L. Vidal, E. Joussein, M. Colas, J. Cornette, J. Sanz, I. Sobrados, J-L.Gelet, J. Absi, S. Rossignol, Controlling the reactivity of silicate solutions: A FTIR, Raman and NMR study, Colloids and Surfaces A: Physicochem. Eng. Aspects, 503 (2016) 101-109.

25. S. Y. R, López and J.S. Rodríguez, Microstructural characterization of sanitaryware by infrared and Raman spectroscopy, the role of vitreous matrix on propierties, J. Ceram. Process. Res., 16 (2015) 162-168.
26. B. O. Mysen, D. Virgo and I. Kushiro, The structural role of aluminum in silicate melts - a Raman spectroscopic study at 1 atmosphere, Am. Mineral., 66 (1981) 678-701.
27. H. Aguiar, J. Serra, P. González, B. León, Structural study of sol–gel silicate glasses by IR and Raman spectroscopies, J. Non-Cryst. Solids, 355 (2009) 475-480.
28. Y. Yu, G. Xiong, C. Li, F.S. Xiao, Characterisation of aluminosilicate zeolites by UV Raman spectroscopy, Microporous Mesoporous Mater., 46 (2001) 23-34.
29. K. Yadav and P. Singh, A review of the structures of oxide glasses by Raman spectroscopy, RSC Adv., 5 (2015) 67583-67609.
30. P. K. Dutta and D.-C.Shieh, Raman spectral study of the composition of basic silicate solutions, Appl. Spectrosc., 39 (1985) 343-346.
31. A. Hajimohammadi, J.L. Provis, J.S.J. van Deventer, The Effect of Silica Availability on the Mechanism of Geopolymerisation, Cem. Concr. Res. 41 (2011) 210-216.
32. Z. Zhang, H. Wang, J.L. Provis, F. Bullen, A. Reid, Y Zhu, Quantitative kinetic and structural analysis of geopolymers. Part1. The activation of metakaolin with sodium hydroxide, Thermochim. Acta, 539 (2012) 23-33.
33. A. Savić, M. Vlahović, S. Martinović, N. Đorđević, G. Broćeta, T. Volkov Husović, Valorization of Fly Ash from a Thermal Power Plant for Producing High-Performance Self-Compacting Concrete, Science of Sintering, 52(2020) 307-327.

Сажетак: *У овом раду, праћена је полимеризација алкално активираног метакаолина (МК) и његове структурне промене, коришћењем 2M NaOH, 8M NaOH и 16M раствора NaOH. Промене су праћене рендгенском фотоелектронском спектроскопијом (XPS), дифузном рефлексијом инфрацрвене Фуријеове трансформације (DRIFT), Рамановом спектроскопијом и скенирајућом електронском микроскопијом (SEM). XPS анализа је показала да промена концентрације NaOH није утицала на типове формираних веза у материјалу. Истовремено, количина натријума и алуминијума се повећавала са моларношћу NaOH. Последњи кораци могу бити посебно интересантни јер могу указивати на могућност 'дозирања' количине Al инкорпорираног променом концентрације NaOH у раствору. DRIFT анализа је открила да је опсег апсорпције за* Al^{IV} *који се налази на 800* cm^{-1} *померен ка мањим вредностима. Променом концентрације NaOH, хемијски садржај се није мењао, али су уочене структурне промене. Раманова спектроскопија је открила да најдоминантнији пикови на 400* cm^{-1} *и 519* cm^{-1} *потичу из Si-O-Al и Si-O-Si начина савијања хемијских веза. Са повећањем концентрације NaOH, пикови на 1019-1060* cm^{-1} *постају све израженији као резултат полимеризације. Обе анализе (DRIFT и Раман) потврдиле су присуство кварца. SEM анализа је показала да се променом концентрације NaOH стварају различите структуре.*

Кључне речи*: метакаолин, геополимер, NaOH, рендгенска фотоелектронска спектроскопија (XPS), Раманова спектроскопија.*